Insights into the Industrial Growth of Cyanobacteria from a Model of the Carbon-Concentrating Mechanism

Ryan L. Clark, Jeffrey C. Cameron, Thatcher W. Root, and Brian F. Pfleger
Dept. of Chemical and Biological Engineering, University of Wisconsin, Madison, WI 53706

DOI 10.1002/aic.14310
Published online January 7, 2014 in Wiley Online Library (wileyonlinelibrary.com)

With the advent of modern bioengineering tools, photosynthetic organisms are increasingly being engineered to produce chemicals from CO_2 sources, thereby creating a potential route of sustainable chemical production. Cyanobacteria have evolved a carbon-concentrating mechanism (CCM) that enables growth at low-environmental carbon concentrations. However at high-carbon concentrations these benefits may not outweigh synthesis costs. Here, mass transport and kinetic modeling analyses were performed on two species of cyanobacteria as well as a hypothetical no-CCM mutant. Modeling results correlated with published experimental data. Three conclusions were drawn from the analysis. Carboxysome geometry was unimportant due to the fast relative rate of diffusion of carbon species. Interspecies variations were largely due to active HCO_3^- transporters. The no-carboxysome cell approaches the wild-type at 10% CO_2. Therefore, in high CO_2 environments the carboxysome and active bicarbonate transporters provide no benefit and a metabolic advantage could be achieved by eliminating the energy-intensive CCM proteins. © 2014 American Institute of Chemical Engineers *AIChE J*, 60: 1269–1277, 2014

Keywords: mass transfer, mathematical modeling, reaction kinetics, environmental engineering, metabolic engineering

Introduction

Sustainable production of fuels and chemicals is a goal of many chemical engineers motivated by economic opportunities and/or environmental concerns. To be sustainable, processes must be developed to recycle and reuse organic materials instead of using finite raw materials such as fossil fuels. Unfortunately, the most abundant source of carbon, atmospheric CO_2, is a poor starting point for most organic syntheses. For this reason, photosynthetic microbes are an attractive biocatalyst platform for converting CO_2 into high-value organic chemicals. Like plants and algae, cyanobacteria have the ability to use sunlight to power the oxidation of water for the generation of cellular energy (ATP) and electrons (reducing equivalents, e.g., NADPH) that can be used to reduce CO_2 and produce organic compounds. To maximize the potential for bioconversion of CO_2 into desirable products, it is useful to understand the fundamental properties and limits of biological CO_2 acquisition and metabolism.

Cyanobacteria are oxygenic photosynthetic microbes found in diverse and often extreme terrestrial, marine, and freshwater environments including the desert, volcanic hot springs, and glaciers.[1] In cyanobacteria, photosynthesis is carried out in the thylakoid membrane, which contains the components of the photosynthetic electron transport chain. The protein complex Photosystem II (PSII) catalyzes the light-driven oxidation of H_2O, producing molecular O_2 as a byproduct. Protons and electrons released during H_2O oxidation are used for ATP production and reduction of $NADP^+$ to NADPH. ATP and NADPH are subsequently utilized by the Calvin-Benson-Bassham cycle (CBB cycle) for the fixation of CO_2 into organic molecules, while O_2 acts as a competitive inhibitor of carbon fixation because of the dual substrate specificity of ribulose 1,5-bisphosphate carboxylase/oxygenase (RuBisCO), the key carbon fixing enzyme.[2]

The slow catalytic turnover and lack of specificity of RuBisCO between CO_2 and O_2 were sufficient for growth under the high concentrations of CO_2 and low concentrations of O_2 in the Earth's early atmosphere. However, over millions of years photosynthetic organisms significantly increased atmospheric O_2 levels and consumed CO_2, shifting their relative abundance.[3] Under current atmospheric conditions (21% O_2 and 0.039% CO_2), CO_2 concentration is a limiting factor for photosynthesis; the photosynthetic capacity of the cell is directly correlated with the availability of CO_2. During the transition from abundant to limiting CO_2 concentrations, cyanobacteria evolved an elaborate CO_2 concentrating mechanism (CCM) comprised of inorganic carbon sequestration systems and the carboxysome, a protein-based organelle for carbon fixation.[4] The CCM functions to concentrate CO_2 at the site of carbon fixation, where it is consumed by RuBisCO. While the CCM is essential for viability in current atmospheric CO_2 concentrations, this requirement can be overcome in laboratory conditions through enrichment of the growth environment in CO_2. In industrial applications using high-CO_2 streams from combustion flue gases, feed enrichment could be as high as 15% CO_2.

In the aqueous environments where cyanobacteria are typically found, HCO_3^- is the predominant form of inorganic carbon (C_i).[5] HCO_3^- is actively transported across the cell by

Correspondence concerning this article should be addressed to B. F. Pfleger at pfleger@engr.wisc.edu.

a suite of membrane bound transporters. Three classes of HCO_3^- transporters have been shown to be important for C_i acquisition in cyanobacteria. BCT1 is a high-affinity ATP binding cassette (ABC) transporter that is induced under low C_i conditions.[6] SbtA is a high affinity, Na^+-dependent transporter that is also induced under low C_i conditions.[7] BicA is a Na^+-dependent, low affinity, high-flux transporter.[8] In *Synechococcus* sp. PCC7002, BicA is present during carbon-replete conditions but is upregulated during carbon limitation. In contrast, the BicA homolog in *Synechocystis* sp. PCC6803 has been reported to be constitutively expressed.[9] Different species of cyanobacteria express some or all of these HCO_3^- uptake systems. *Synechocystis* sp. PCC6803 contains all three systems, while *Synechococcus elongatus* PCC7942 lacks BicA, and *Synechococcus* PCC7002 lacks BCT1.[8] Moreover, differences in transport activity have been reported for the BicA homologs.[8] In contrast to HCO_3^-, CO_2 is able to diffuse across the cell membrane. Two CO_2 uptake protein complexes, NDH-1_4 and NDH-1_3, are involved in the hydration of CO_2 into HCO_3^- in the cytoplasm.[10] NDH-1_4 is a constitutively expressed, low-affinity uptake system that may be located on the plasma membrane[11,12]. NDH-1_3 is a high-affinity, low C_i inducible system located on the thylakoid membrane.[11–13] The concerted activity of these transporters allows the cells to accumulate high-internal levels of HCO_3^-.

In addition to the C_i acquisition system, the CCM also requires the carboxysome, which is a protein-based bacterial microcompartment (BMC) in cyanobacteria that resembles an icosahedral viral capsid.[14] It is composed of a semipermeable shell containing hexameric and pentameric proteins surrounding RuBisCO and carbonic anhydrase (CA)[15] in the interior. The shell has been proposed to be permeable to HCO_3^-, but not O_2 or CO_2 due to the electrostatic properties of the residues lining the pore of each shell protein.[16] Once HCO_3^- enters the carboxysome, it is dehydrated to create CO_2, to provide the substrate for RuBisCO. This process is catalyzed by CA, known to be one of the most active enzymes.[17] RuBisCO catalyzes the carboxylation of ribulose 1, 5-bisphosphate (RuBP) to form two molecules of 3-phosphoglycerate (3-PGA). 3-PGA diffuses out of the carboxysome, where it is consumed by the CBB-cycle, providing the major sink for photosynthetically derived ATP and NADPH. Carboxysomes are found in all free-living cyanobacteria and are essential for survival in ambient CO_2 concentrations. However, they are dispensable at high-CO_2 (e.g., 3%) concentrations. Thus, strains lacking a carboxysome have a high-CO_2 requiring (HCR) phenotype.[18] It is critical to the formation of the intracellular HCO_3^- pool that CA activity is localized exclusively to the carboxysome. It has been shown that expression of an extra-carboxysomal human CA in *Synechococcus elongatus* PCC7942 results in an HCR phenotype.[19] Evidence suggests that this locational specificity is accomplished through deactivation of carboxysomal CA before it is oxidized during carboxysome biogenesis.[20]

The CCM provides significant fitness benefits to the cell during natural, low-CO_2 conditions. However, it is not clear whether the CCM will be beneficial in an industrial setting with a concentrated CO_2 stream such as flue gas as a feedstock for photosynthetic production of fuels and chemicals. Previously, several groups have investigated the maximum CO_2 fixation rates in cyanobacteria and the role of the CCM.[8,21] However, equivalent models have not been used to investigate the maximum CO_2 fixation rates in carboxysome-less strains exposed to different C_i concentrations. In this work, we investigate the effects of diffusion, size and number of carboxysomes, and the active carbon uptake system on rates of photosynthesis. Our results provide insight into the limitations of carbon fixation and the strategies for increased carbon fixation in industrially relevant conditions.

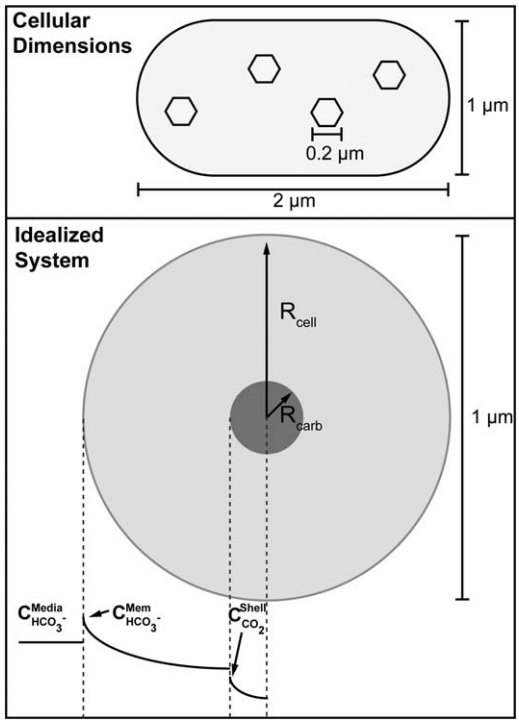

Figure 1. Spherical approximations were made for the model of the wild-type cyanobacteria.

The HCO_3–profile is exaggerated to emphasize any concentration gradients needed to produce diffusive flux to the carboxysome. The same spherical boundary at the membrane was used in the model of the carboxysome-lacking mutant.

Definition of Model

Simplifying assumptions that eliminate unimportant parameters and emphasize the question at hand are at the heart of any transport analysis in the style of Bird, Stewart, and Lightfoot. In this study, we investigated the impact of the carbon-concentrating mechanism evolved by cyanobacteria on the rate of carbon-fixation by RuBisCO over a range of industrially relevant CO_2 concentrations. The simplifications imposed upon this problem address geometry, kinetics, and mass transport. To demonstrate the importance and impact of the CO_2 concentrating mechanism, two cases were considered: A wild type cyanobacterium and a mutant lacking the carboxysome unit of the CCM. Quantitative results were obtained by applying this analysis to two different species of cyanobacteria (1) the industrially attractive *Synechococcus sp.* PCC 7002, and (2) the model strain for studies of β-carboxysomes, *Synechococcus elongatus* PCC 7942.

For modeling purposes, the geometry of the cyanobacterial cell was idealized to a sphere in a well-mixed medium as shown in Figure 1, resulting in a problem analogous to the classic "Diffusion and Chemical Reaction Inside a Porous Catalyst" problem.[22] The membranes of the cell were assumed to be negligible in thickness relative to the radius of the cell and form the outer boundary of the sphere. The

permeability of lipid bilayers to CO_2 is six-orders of magnitude higher than to HCO_3^-, so the cell membrane was assumed HCO_3^- -impermeable.[23]

For the wild-type case, the cell was divided into two distinct phases: the carboxysome and the cytoplasm. Convective velocities within the cell were assumed to be negligible, leaving mass transport to occur only through diffusion. BicA is the most relevant active carbon transporter in PCC 7002 in the CO_2 concentration range studied in this analysis and was, therefore, the only transporter considered. PCC 7942 does not have a BicA transporter so we chose to estimate its HCO_3^- flux as a fraction of that of PCC 7002 determined from the literature.[8] The consumption of CO_2 and HCO_3^- in the cytoplasm by non-carbon-fixation related metabolic processes was considered negligible relative to carbon-fixation catalyzed by RuBisCO. At the inner boundary of the cytoplasm phase located at the carboxysome wall, a Fick's Law constant flux boundary condition was imposed. The flux into the carboxysome was the integrated CO_2 consumption rate inside the carboxysome per unit surface area of the carboxysome.

The cell was modeled with one concentric spherical carboxysome within which the consumption of CO_2 occurred through a homogeneous reaction catalyzed by uniformly packed RuBisCO. The O_2-inhibited Michaelis-Menten kinetic model[24] was used for the carbon fixation rate of RuBisCO

$$v=\frac{k_{cat}[R]C_{CO_2}^{Carb}}{C_{CO_2}^{Carb}+K_{m,CO_2}\left(1+\frac{C_{O_2}^{Carb}}{K_{m,O_2}}\right)} \tag{1}$$

The k_{cat} for carbonic anhydrase[17] present in the carboxysome is four orders of magnitude larger than that of RuBisCO,[25] so HCO_3^- was treated as instantaneously equilibrated with CO_2 within the carboxysome. Therefore, the concentration of CO_2 directly inside the carboxysome wall was proportional to the HCO_3^- concentration directly outside of the wall in the cytoplasm phase. The proportionality constant incorporated both the CO_2-HCO_3^- equilibrium constant and a barrier to HCO_3^- transport across the carboxysome wall. Evidence suggesting a mechanism to prevent the leakage of CO_2 from the carboxysome exists, so the carboxysome wall was approximated as impermeable to CO_2.[4]

The second case considered a mutant cyanobacterial cell lacking the carboxysomes and active bicarbonate transporters, with a mutant model simplified by two primary differences from the wild type. First, RuBisCO was considered to be distributed homogeneously throughout the single cytoplasm phase. Second, the CO_2 concentration was determined only by direct diffusion across the cell membrane.

Transport Analysis

To determine the importance of diffusion in the carbon fixation process, the differential mass balances for the various phases in question were examined. The balances were nondimensionalized and the reactive flux was compared to the diffusive flux. The resulting dimensionless group, referred to as the Damköhler number, is defined as the ratio of the characteristic reaction rate to the characteristic diffusion rate for each case.[26] This analysis focuses on fluxes of CO_2 and HCO_3^- as key species controlling the RuBisCO carbon fixation kinetics. This step also involves consumption of coreactants and generation of products, including RuBP, 3-PGA, ATP, and NADH. These need not be modeled explicitly because they are also small molecules that would be present at excess concentrations as provided by other processes and would be expected to have diffusive properties[27,28] almost as fast as CO_2. Furthermore, these species have not been observed to affect RuBisCO reaction rates under nutritionally sufficient conditions.

CO_2 in Carboxysome

In considering the CO_2 profile inside the carboxysome, the differential mass balance equation for a sphere with homogeneous reaction following oxygen-inhibited Michaelis-Menten kinetics was used with constant surface concentration and spherical symmetry boundary conditions

$$\frac{D_{CO_2}^{Carb}}{r^2}\frac{\partial}{\partial r}\left(r^2\frac{\partial C_{CO_2}^{Carb}}{\partial r}\right)=\frac{k_{cat}[R]C_{CO_2}^{Carb}}{C_{CO_2}^{Carb}+K_{m,CO_2}\left(1+\frac{C_{O_2}^{Carb}}{K_{m,O_2}}\right)} \tag{2}$$

$$BC1: C_{CO_2}^{Carb}=C_{CO_2}^{Shell} \quad \text{at} \quad r=R_{Carb} \tag{3}$$

$$BC2: \frac{\partial C_{CO_2}^{Carb}}{\partial r}=0 \quad \text{at} \quad r=0 \tag{4}$$

where $C_{CO_2}^{Shell}$ is related to the HCO_3^- concentration in the cytoplasm by a function unimportant for the transport analysis. This relationship was revisited in the kinetic analysis of the localization of CO_2 to the carboxysome for carbon fixation.

For further simplification, two situations were considered for the rate expression of the RuBisCO catalyzed reaction: one in which $C_{CO_2}^{Carb} \gg K_{m,CO_2}$, resulting in zero-order kinetics, and one in which $C_{CO_2}^{Carb} \ll K_{m,CO_2}$, resulting in first-order kinetics. For nondimensionalizing these equations, the characteristic length used was the carboxysome radius and the characteristic concentration used was the CO_2 concentration at the carboxysome surface. The following Damköhler numbers were determined

$$C_{CO_2}^{Carb} \gg K_{m,CO_2}: \quad Da=\frac{k_{cat}[Ru]_{Carb}R_{Carb}^2}{D_{CO_2}^{Carb}C_{CO_2}^{Shell}} \tag{5}$$

$$C_{CO_2}^{Carb} \ll K_{m,CO_2}: \quad Da=\frac{k_{cat}[Ru]_{Carb}R_{Carb}^2}{D_{CO_2}^{Carb}K_{m,CO_2}\left(1+\frac{C_{O_2}^{Carb}}{K_{m,O_2}}\right)} \tag{6}$$

The inorganic carbon flux at the carboxysome shell was needed for transport analysis of the cytoplasm phase. Expressions for J^* were determined for zero- and first-order kinetics by integrating the rate expressions over the volume of the carboxysome and dividing by the surface area of the carboxysome, resulting in the following expressions

$$C_{CO_2}^{Carb} \gg K_{m,CO_2}: \quad J^*=\frac{k_{cat}[Ru]_{Carb}R_{Carb}}{4} \tag{7}$$

$$C_{CO_2}^{Carb} \ll K_{m,CO_2}: \quad J^*=\frac{k_{cat}[Ru]_{Carb}R_{carb}C_{CO_2}^{Shell}}{3K_{m,CO_2}} \tag{8}$$

HCO_3^- in Cytoplasm. The HCO_3^- profile within the cytoplasm of the wild type cell was calculated from the spherical differential mass balance equation with no generation or consumption term. A constant concentration boundary condition was applied at the cell membrane boundary, and a constant flux boundary condition was applied at the carboxysome boundary

$$\frac{\partial}{\partial r}\left(r^2\frac{\partial C_{HCO_3^-}^{Cyt}}{\partial r}\right)=0 \tag{9}$$

Table 1. Values used to Calculate Damköhler Numbers

Variable	Value/Estimate	Rationale	Citation
Specified Values			
k_{cat}	11.4 $s^{-1} \cdot site^{-1}$	Value for RuBisCO isolated from PCC 7002	25
K_{m,CO_2}	185 $\frac{\mu mol}{L}$	Value for RuBisCO isolated from PCC 7002	25
K_{m,O_2}	1300 $\frac{\mu mol}{L}$	Value for RuBisCO isolated from PCC 7002	25
R_{Carb}	100 nm	Radius of a carboxysome in PCC 7942	21
Values in the Numerator of Damköhler Numbers (Maximum Limit)			
$[Ru]_{Carb}$	10^{-3} $\frac{site}{nm^3}$	Wild Type: The inverse volume of one unit of RuBisCO	32
$[Ru]_{Cyt}$	10^{-6} $\frac{site}{nm^3}$	No Carboxysome: RuBisCO from carboxysome distributed uniformly throughout cytoplasm	32
$\frac{C^{Shell}_{CO_2}}{C^{Mem}_{HCO_3^-}}$	0.01	Equilibrium concentration is $\frac{10^{-pH}}{K_a}$ at pH=8, Temperature= 38°C	5
R_{Cell}	1000 nm	Approximated spherical radius of a PCC 7942 cell (Larger than PCC 7002)	30,33
Values in the Denominator of Damköhler Numbers (Minimum Limit)			
D^j_i	3×10^{-6} $\frac{cm^2}{s}$	Diffusivity of a small molecule in cytoplasm	28
$C^{Mem}_{CO_2}$ or $C^{Shell}_{CO_2}$	185 $\frac{\mu mol}{L}$	For excess carbon, concentration must be at least equal to the affinity constant	25
C_{O_2}	0 $\frac{\mu mol}{L}$	Rate is maximized in absence of O_2 inhibition	-
$C^{Mem}_{HCO_3^-}$	10 $\frac{\mu mol}{L}$	1000 times lower than equilibrium concentration at atmospheric conditions.	5

$$BC1: C^{Cyt}_{HCO_3^-} = C^{Mem}_{HCO_3^-} \quad \text{at} \quad r = R_{Cell} \tag{10}$$

$$BC2: \frac{\partial C^{Cyt}_{HCO_3^-}}{\partial r} = \frac{-J^*}{D^{Cyt}_{HCO_3^-}} \quad \text{at} \quad r = R_{Carb} \tag{11}$$

where $C^{Mem}_{HCO_3^-}$ is related to the HCO_3^- concentration in the media by a flux balance unimportant for the transport analysis. This relationship was revisited in the kinetic analysis of the formation of the intracellular HCO_3^- pool.

For the cytoplasm phase, the characteristic length was the radius of the cell and the characteristic concentration was the HCO_3^- concentration at the inside of the cell membrane interface. The solution to this nondimensionalized differential mass balance and its boundary conditions resulted in the following Damköhler number relating the rate of reaction to the rate of diffusive flux

$$Da = \frac{J^* R^2_{Carb}}{D^{Cyt}_{HCO_3^-} C^{Mem}_{HCO_3^-} R_{cell}} \tag{12}$$

The expressions for J^* determined in the analysis of the carboxysome phase were used to determine the final Damköhler numbers for the cases of $C^{Carb}_{CO_2} \gg K_{m,CO_2}$ and $C^{Carb}_{CO_2} \ll K_{m,CO_2}$.

No-carboxysome case

The differential mass balance and boundary conditions for the mutant case of a cell with no carboxysomes were analogous to the carboxysome phase of the previous case. The characteristic length for this case was the radius of the cell and the characteristic concentration was the CO_2 concentration at the cell membrane interface, which was equal to the CO_2 concentration in the media. The resulting Damköhler numbers were as follows

$$C^{Cyt}_{CO_2} \gg K_{m,CO_2}: \quad Da = \frac{k_{cat}[Ru]_{Cyt} R^2_{Cell}}{D^{Cyt}_{CO_2} C^{Mem}_{CO_2}} \tag{13}$$

$$C^{Cyt}_{CO_2} \ll K_{m,CO_2}: \quad Da = \frac{k_{cat}[Ru]_{Cyt} R^2_{Cell}}{D^{Cyt}_{CO_2} K_{m,CO_2}\left(1 + \frac{C^{Cyt}_{O_2}}{K_{m,O_2}}\right)} \tag{14}$$

Determination of controlling phenomena

The numerical values of the Damköhler numbers allow assessment of relative importance of transport and reaction rates in limiting overall carbon fixation. If Da $\approx$ 1, both reaction and diffusion are comparable, and as Da differs more from unity then the slower process completely controls the overall rate. A range of parameter values can be found in the literature, and preliminary evaluation showed Da $\ll$ 1 to indicate reaction is generally slow compared to diffusion. To test how close the Damköhler numbers approached the Da $\approx$ 1 regime in which diffusion is not rapid, extreme high- and low-parameter values were chosen to maximize the Damköhler number. The values used in the calculation as well as their rationale can be found in Table 1. The constants associated with the RuBisCO kinetics specific to PCC 7002 were used in this analysis. However, many other species have k_{cat} and K_m values within an order of magnitude of these values so the result was applied to PCC 7942 and may be applied in a somewhat general way.[25] The expressions and extremal values associated with each Damköhler number can be seen in Table 2 and each was of an order of magnitude smaller than 10^{-3}.

Because these Da values are all so small, diffusive processes are all fast compared to reaction rates and the HCO_3^- and CO_2 concentrations can be treated as constant across each phase. Therefore, the carbon fixation rate is independent of the number or size of carboxysomes at a fixed total number of RuBisCO units per cell. In the no-carboxysome case, rapid diffusion will provide a constant CO_2 concentration inside the cell independent of the HCO_3^- concentration or the kinetics of the conversion between HCO_3^- and CO_2. Thus, the presence or absence of active HCO_3^- transporters in the no-carboxysome cell has no effect and the activity of the carbonic anhydrase, which has been postulated to be

Table 2. Summary of Damköhler Numbers

Case	Phase	Conditions	Damköhler Number	Estimated Value
Wild Type	Cyt	$C_{CO_2}^{Cyt} \gg K_{m,CO_2}$	$\frac{k_{cat}[Ru]_{Carb}R_{Carb}^3}{4D_{HCO_3^-}^{Cyt}C_{HCO_3^-}^{Mem}R_{Cell}}$	2×10^{-3}
Wild Type	Carb	$C_{CO_2}^{Carb} \gg K_{m,CO_2}$	$\frac{k_{cat}[Ru]_{Carb}R_{Carb}^2}{D_{CO_2}^{Carb}C_{CO_2}^{Shell}}$	3×10^{-3}
Wild Type	Cyt	$C_{CO_2}^{Cyt} \ll K_{m,CO_2}$	$\frac{k_{cat}[Ru]_{Carb}R_{Carb}^3\left(\frac{C_{CO_2}^{Shell}}{C_{HCO_3^-}^{Mem}}\right)}{3K_{m,CO_2}D_{HCO_3^-}^{Cyt}R_{Cell}}$	1×10^{-6}
Wild Type	Carb	$C_{CO_2}^{Carb} \ll K_{m,CO_2}$	$\frac{k_{cat}[Ru]_{Carb}R_{Carb}^2}{D_{CO_2}^{Carb}K_{m,CO_2}\left(1+\frac{C_{O_2}^{Carb}}{K_{m,O_2}}\right)}$	3×10^{-3}
No Carboxysome	Cyt	$C_{CO_2}^{Cyt} \gg K_{m,CO_2}$	$\frac{k_{cat}[Ru]_{Cyt}R_{Cell}^2}{D_{CO_2}^{Cyt}C_{CO_2}^{Mem}}$	3×10^{-4}
No Carboxysome	Cyt	$C_{CO_2}^{Cyt} \ll K_{m,CO_2}$	$\frac{k_{cat}[Ru]_{Cyt}R_{Cell}^2}{D_{CO_2}^{Cyt}K_{m,CO_2}\left(1+\frac{C_{O_2}^{Cyt}}{K_{m,O_2}}\right)}$	3×10^{-4}

inactive outside of the carboxysome environment,[20] does not affect these calculations.

Kinetic Analysis

A kinetic approach was utilized to determine a quantitative explanation of carbon fixation in cyanobacterial cells. Figure 2 shows a schematic diagram of the processes occurring during steady-state carbon uptake and Table 3 gives the equations used to model these processes. These processes can be divided into three different stages (1) external CO_2 equilibrium, (2) inorganic carbon uptake, and (3) carbon fixation.

External CO_2 equilibrium

The first stage of carbon uptake is concerned with the transfer of carbon from the gas phase to the liquid phase. The CO_2 concentration in the liquid phase was determined from a Henry's Law relationship with a gas phase at 1 atm and variable CO_2 concentration. The liquid phase was considered well-mixed so that CO_2 and HCO_3^- were at chemical equilibrium[5] in the liquid

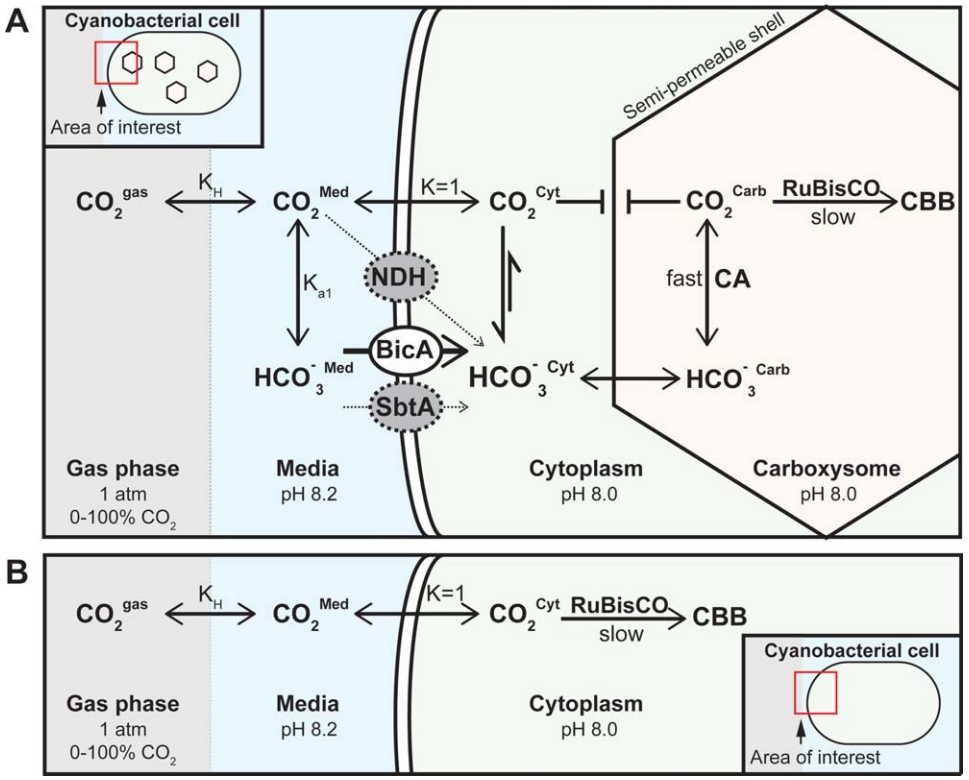

Figure 2. Kinetic model used to calculate carbon flux into the CBB-cycle.

(A) The schematic for the wild-type cell containing the entire CCM (The NDH and SbtA inorganic carbon transporters have small flux compared to BicA and were neglected), and (B) the schematic for the carboxysome-lacking mutant. The equations used to model the reactions in these schematics are given in Table 3. [Color figure can be viewed in the online issue, which is available at wileyonlinelibrary.com.]

Table 3. Kinetics Model of Inorganic Carbon Uptake

Process	Equation	Literature Values	Citation
Wild Type Cyanobacteria			
$CO_2^{Gas} \overset{K_H}{\leftrightarrow} CO_2^{Med}$	$C_{CO_2}^{Med} = P_{CO_2} K_H$	$K_H = 0.02 \ \frac{mol}{L \cdot atm}$	5
$H_2O + CO_2^{Med} \overset{K_a}{\leftrightarrow} HCO_3^{-Med} + H^{+Med}$	$C_{H^+}^{Med} C_{HCO_3^-}^{Med} = K_a C_{CO_2}^{Med}$	$K_a = 0.9 \ \frac{\mu mol}{L}$	5
$CO_2^{Med} \leftrightarrow CO_2^{Cyt}$	$C_{CO_2}^{Cyt} = C_{CO_2}^{Med}$	Permeability $CO_2 >> HCO_3^-$	23
$HCO_3^{-Med} \xrightarrow{BicA} HCO_3^{-Cyt}$	$v_{in} = \frac{v_{max} C_{HCO_3^-}^{Med}}{K_m + C_{HCO_3^-}^{Med}}$	$v_{max} = 0.4 \frac{\mu mol}{mg \ Chl \ a \cdot s} = 4 \times 10^9 \frac{molecules}{cell \cdot hr}$ $K_m = 217 \frac{\mu mol}{L}$	8[a]
$CO_2^{Cyt} + OH^{-Cyt} \overset{k_f, k_r}{\Longleftrightarrow} HCO_3^{-Cyt}$	$v_f = k_f C_{CO_2}^{Cyt} C_{OH^-}^{Cyt}$ $v_r = k_r C_{HCO_3^-}^{Cyt}$	$k_f = 3 \times 10^4 \frac{L}{mol \cdot s}$ $k_r = 1 \times 10^{-3} s^{-1}$	29
$HCO_3^{-Cyt} \overset{Q}{\leftrightarrow} HCO_3^{-Carb}$	$C_{HCO_3^-}^{Carb} = Q C_{HCO_3^-}^{Cyt}$	$Q \sim 1$	-
$HCO_3^{-Carb} + H^{+Carb} \overset{CA}{\leftrightarrow} H_2O + CO_2^{Carb}$	$K_a C_{CO_2}^{Carb} = C_{H^+}^{Carb} C_{HCO_3^-}^{Carb}$	$k_{cat}^{CA} \sim 10^4 \cdot k_{cat}^{Rub}$, Fast Equilibrium	17,25
$CO_2^{Carb} \xrightarrow{RuBisCO} CBB \ Cycle$	$v_{fix} = \frac{k_{cat} N_{sites} C_{CO_2}^{Carb}}{C_{CO_2}^{Carb} + K_{m,CO_2}\left(1 + \frac{C_{O_2}^{Carb}}{K_{m,O_2}}\right)}$	$k_{cat} = 11.4 \ \frac{molecules}{site \cdot s}$ $K_{m,CO_2} = 185 \ \frac{\mu mol}{L}$ $K_{m,O_2} = 1300 \ \frac{\mu mol}{L}, [O_2] = 400 \frac{\mu mol}{L}$ $N_{sites} = \left(4 \frac{carboxysomes}{cell}\right)\left(3351 \frac{sites}{carboxysome}\right)$	34–36
No Carboxysome Mutant			
$CO_2^{Gas} \overset{K_H}{\leftrightarrow} CO_2^{Med}$	$C_{CO_2}^{Med} = P_{CO_2} K_H$	$K_H = 0.02 \ \frac{mol}{L \cdot atm}$	5
$CO_2^{Med} \leftrightarrow CO_2^{Cyt}$	$C_{CO_2}^{Cyt} = C_{CO_2}^{Med}$	Permeability $CO_2 >> HCO_3^-$	23
$CO_2^{Carb} \xrightarrow{RuBisCO} CBB \ Cycle$	$v_{fix} = \frac{k_{cat} N_{sites} C_{CO_2}^{Carb}}{C_{CO_2}^{Carb} + K_{m,CO_2}\left(1 + \frac{C_{O_2}^{Carb}}{K_{m,O_2}}\right)}$	$k_{cat} = 11.4 \ \frac{molecules}{site \cdot s}$ $K_{m,CO_2} = 185 \ \frac{\mu mol}{L}$ $K_{m,O_2} = 1300 \ \frac{\mu mol}{L}, [O_2] = 400 \frac{\mu mol}{L}$ $N_{sites} = \left(4 \frac{carboxysomes}{cell}\right)\left(3351 \frac{RuBisCo}{carboxysome}\right)$	34–36

[a]Chlorophyll content of PCC 7002 cells were measured to be $5 \times 10^{-12} \frac{mg \ Chl \ a}{cell}$ during exponential growth phase as in Lichtenthaler[37]

phase. The equilibrium inorganic carbon concentrations calculated for any gas-phase concentration are the maximum possible achievable. This ideality may not hold in the laboratory for most situations and this stage could be adjusted to fit various bioreactor geometries and transport scenarios.

HCO_3^- uptake

The second stage in carbon uptake is concerned with the formation of an intracellular bicarbonate pool through the transfer of carbon from the liquid media to the cytoplasm of the cell. This stage has the largest interspecies variation as the active transport systems utilized by β-cyanobacteria vary from species to species. In PCC 7002, the primary HCO_3^- transporter BicA has a flux that is orders of magnitude higher than any of the other transporters, and as these processes are parallel they do not contribute significantly to the carbon flux.[8] PCC 7942 lacks this BicA transporter and thus has significantly lower flux of carbon into the cell. In a study by Price et al, the BicA transporter from PCC 7002 was introduced into PCC 7942 and an approximately tenfold increase in maximum carbon flux was observed.[8] Therefore, in the model for PCC 7942, the HCO_3^- flux expression from the PCC 7002 model was used with a V_{max} equal to 10% of that used for PCC 7002.

Once inside the cell, HCO_3^- is only slowly dehydrated to CO_2 in an uncatalyzed process due to the absence of carbonic anhydrase in the cytoplasm.[29] The slow rate of this conversion is crucial to the formation of the inorganic carbon pool. As the cell membrane is essentially impermeable to HCO_3^-, a high concentration of HCO_3^- is trapped inside the cell. The cell membrane presents no barrier to the transfer of CO_2 so any HCO_3^- that is converted to CO_2 leaks out of the cell into the media, equilibrating the outer and inner CO_2 concentrations.

Carbon fixation

The third stage in carbon uptake is the localization of carbon to the carboxysome where it can be consumed by RuBisCO. This is the most controversial of the steps studied in the carbon-concentrating mechanism. It is not known how HCO_3^- passes into the carboxysome or if there is a barrier to this flux. In order to approximate the concentration of HCO_3^- in the

carboxysome relative to that in the cytoplasm, a proportionality relationship was established between the HCO_3^- inside and outside of the carboxysome. The proportionality constant Q was initially set to 1.0 to evaluate the upper limit of the carbon fixation rate and the sensitivity of the model to decreases in this parameter was examined. The model was not overly sensitive to the value of Q within an order of magnitude, so the original value of 1 was used for further analysis.

The HCO_3^- inside the carboxysome was treated as quickly equilibrated with CO_2 by carbonic anhydrase.[17,25] The carboxysome was considered impermeable to CO_2 as it has been generally hypothesized that that the protein shell prevents its escape.[4] The RuBisCO catalyzed reaction in which CO_2 flux is directed into the Calvin Cycle was used as the rate determining step in the reaction scheme, based on the earlier Da analysis. There was postulated to be an excess of ribulose-1,5-bisphosphate, the cosubstrate required for carbon fixation by RuBisCO. It is expected that the kinetic values for RuBisCO in PCC 7002 and PCC 7942 are within an order of magnitude of each other, as is the trend with other strains of cyanobacteria.[25]

Solving the reaction system

To determine the carbon uptake rate of the cell, the rate equation for RuBisCO catalyzed fixation of CO_2 was used as the rate-limiting step with the rapid diffusion and active transport steps proceeding as outlined peviously. The key to solving the reaction system was equating the flux into and out of the cell's HCO_3^- pool. This expression is as follows

$$\begin{pmatrix} Active\ HCO_3^- \\ Pump\ Flux \end{pmatrix} = \begin{pmatrix} Carbon\ Consumption \\ by\ RuBisCo \end{pmatrix} + \begin{pmatrix} Net\ Conversion\ of \\ HCO_3^-\ to\ CO_2 \end{pmatrix} \tag{15}$$

$$\left(\frac{v_{max}C^{Media}_{HCO_3^-}}{K_{m,HCO_3^-}+C^{Media}_{HCO_3^-}}\right) = \left(\frac{k_{cat}N_{sites}C^{Carb}_{CO_2}}{C^{Carb}_{CO_2}+K_{m,CO_2}\left(1+\frac{C^{Carb}_{O_2}}{K_{m,O_2}}\right)}\right) + [(k_rC^{Cyt}_{HCO_3^-}-k_fC^{Cyt}_{CO_2}C^{Cyt}_{OH^-})V_{cell}] \tag{16}$$

where the first term represents the flux into the cell due to active HCO_3^- transport, the second term represents the forward reaction of CO_2 into HCO_3^-, the third term represents the flux of carbon into the CBB-cycle, and the final term represents the reverse reaction of HCO_3^- into CO_2. This expression was solved analytically for the CO_2 concentration inside the carboxysome and the carbon fixation rate as a function of $C^{Media}_{HCO_3^-}$ can be seen in Figure 3 for each cyanobacterial species. The resulting curves were compared to oxygen evolution data obtained from literature[8,21] for wild type strains of each species with good agreement in trend. Oxygen evolution rate is proportional to carbon fixation rate because the CBB-cycle acts as a sink for energy and reducing power generated during photosynthesis.[2]

No-carboxysome case

The reaction scheme for the hypothetical case of a cell with no carboxysomes, depicted in Figure 2, was much simpler than that of the wild-type case. This model was solved analytically and the resulting carbon fixation rate as a function of can be seen in Figure 3 for comparison to the wild-type case. As expected, the model predicts that both cyanobacterial species have little or no carbon fixation activity at present ambient CO_2 levels, and shows the clear necessity of the CCM in wild-type species. However, CO_2 transport without HCO_3^- pumping allows significant CCM at gas phase CO_2 compositions of 10% or greater. Thus, the carboxysome may become unnecessary at sufficient CO_2 levels. Indeed, PCC 7942 models show the carboxysome-free variant predicted to have a higher carbon fixation rate over a range of enriched CO_2 levels.

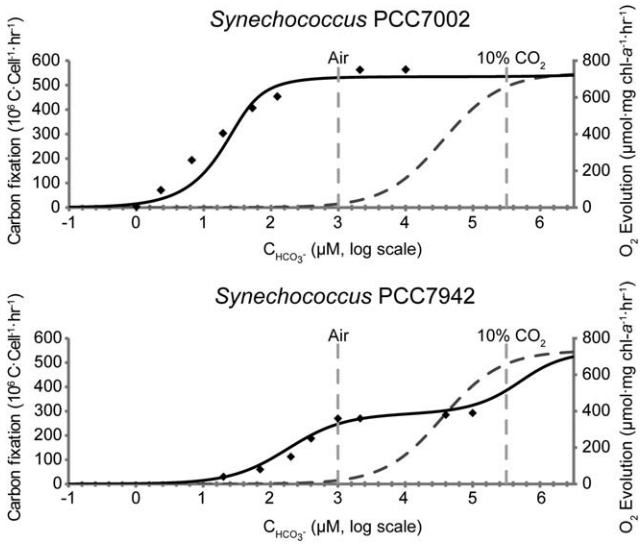

Figure 3. Plots of potential carbon fixation rate as a function of the inorganic carbon concentration in the media for the wild-type (solid line) and carboxysome-lacking mutant (dashed line) for both PCC 7002 and PCC 7942.

The vertical lines indicate HCO3- concentrations achievable in the media through equilibrium with a gas phase containing CO_2 at concentrations of 400 ppm (air) and 10% (flue gas). Points (◆) represent data from the literature (8,21) showing O_2 evolution in wild-type cultures of each species as a function of media HCO_3^- concentration with corresponding values on the righthand *y*-axis.

Discussion

Three important conclusions can be drawn from this study. First, carbon uptake is not diffusion limited, so the number, size, shape, and intracellular location of the carboxysomes have a negligible effect on carbon fixation rate with a given number of RuBisCO units and these details need not be considered further. Second, large interspecies variations in the carbon fixation landscape are largely due to the difference in the kinetics of the active HCO_3^- transporters present in the cell. Finally, the potential carbon fixation rate of the no-carboxysome cell approaches and can even surpass that of the wild type when grown at CO_2 concentrations of 10% or higher. These conclusions were considered in their implications on future research paths.

Carboxysome engineering

At gas phase CO_2 concentrations approaching that of flue gas, there is not a large carbon fixation benefit in a cell containing carboxysomes. In the low HCO_3^- flux case of PCC 7942, there was even a carbon fixation deficit as the cytoplasmic CO_2 concentration due to a high media

concentration overcomes that achievable by the carbon concentrating mechanism and the carboxysome serves only as a barrier to the localization of CO_2 to RuBisCO. Because the carboxysome shell proteins are very large with a final structure diameter on the order of 10% of that of the cell, there would be a metabolic benefit in redirecting the energy used to make these proteins as well as others involved in the CCM into other processes, such as the production of more RuBisCO units.[21,30] This would be an interesting area of research to increase a cell's affinity to the high CO_2 environments relevant to industrial processes. The natural elimination of carboxysomes at high CO_2 concentrations has been observed in at least one wild type cyanobacterium.[31] Another benefit of the removal of carboxysomes from a genetically modified cyanobacterial strain would be to reduce its fitness in nature so it is unable to grow in ambient CO_2 levels, mitigating the possibility of inadvertent release and potential biological contamination of the environment by genetically modified organisms.

HCO_3^- *transporter engineering*

As the carbon-fixation rate of RuBisCO reaches saturation at low concentrations for high HCO_3^- flux species such as PCC 7002, increasing the affinity or flux of these transporters will not provide a benefit. However, in low HCO_3^- flux species such as PCC 7942, a great carbon fixation benefit at all CO_2 levels should be achieved by the introduction of a higher flux HCO_3^- transporter. The potential magnitude of this benefit is especially evident when comparing the accepted doubling times of 4 h for PCC 7002 to 10 hours for PCC 7942.[8,21] The benefit of the implementation of the high-flux HCO_3^- transporter BicA from PCC7002 in PCC 7942 has been observed.[8]

RuBisCO engineering

The modification of RuBisCO for increased performance has long been a goal of researchers who desire to increase the efficiency of photosynthesis.[32] There are two targets relevant to this model for increasing the performance of RuBisCO: k_{cat} and affinity. Increasing the k_{cat} of RuBisCO will naturally increase the carbon fixation rate of a cell. This rate of increase will be approximately linear in the case of a high flux cell or the hypothetical no-carboxysome cell as the enzyme will be saturated until the k_{cat} is increased by an order of magnitude. In the case of a low-flux cell, increases to the of RuBisCO do not have as large of a carbon fixation benefit as the saturation of the active bicarbonate transporters prevents RuBisCO saturation.

Increasing the affinity of RuBisCO for CO_2 can greatly improve the carbon fixation rate of the no-CCM case by allowing for RuBisCO saturation at lower CO_2 concentrations. This same benefit could be achieved in the low HCO_3^- flux PCC 7942 cell, but this effect is not addictive when compared to the effect of improved active HCO_3^- transport. Little benefit will be achieved by this affinity increase in the high HCO_3^- flux PCC 7002 cell, as the RuBisCO is already saturated by the significantly higher CO_2 concentration at industrially relevant CO_2 concentrations.

Conclusion

A mass-transport model considering the uptake of inorganic carbon by cyanobacteria showed that diffusion was fast compared to kinetic conversion by RuBisCO yielding flat CO_2 and HCO_3^- concentration profiles within the cell. As a result, the number, size, shape, and intracellular location of carboxysomes have a negligible effect on carbon fixation rate with a given number of RuBisCO units. A kinetic model of the fluxes of inorganic carbon in the carbon uptake systems of wild-type and hypothetical carboxysome-lacking mutant cyanobacteria was developed. The wild-type case for both PCC 7002 and PCC 7942 matched the trend of experimental oxygen-evolution data from the literature. Interspecies variations in the potential carbon-fixation rate are largely due to differences in active HCO_3^- transporters. The models showed that the potential steady-state carbon-fixation rate of a carboxysome-lacking mutant approaches that of the wild type at inorganic carbon concentrations achievable using a gas feed containing 10% CO_2. Future research towards increasing the fitness of cyanobacteria in an industrial setting should focus on the metabolic benefits of the elimination of the energy-intensive proteins associated with the CCM that are not necessary at high CO_2 concentrations.

Acknowledgments

This article is dedicated to Bob Bird, who has inspired us in many different ways. His clarity of thought and focus on key fundamentals have been signal features in his research, teaching, and writing. Authorship of several landmark textbooks provides lasting impact on generations of new chemical engineers. Neatness and organization permeated his presentations, so his course lectures were widely appreciated by students and colleagues and were a central demonstration of his love of teaching. Knighthood conveyed by Queen Beatrice in recognition of his activity with the UW Dutch Club is an indication of his commitment to languages and culture. Students from many countries have been surprised and pleased to be greeted by Bob in their native tongues. But Bob's recreational interests, ranging from languages to canoe voyages to hidden messages, puzzles, and limericks, also enriched and entertained all he encountered. One such canoe trip with colleagues in 1989 may have provided an early exposure to algae for one author (TWR) and the father of another (DCC/JCC), and in some way led to this paper. Both in his vocation and his avocations, we can say that Bob exemplifies "Mighty Good Stuff".

This algae's a wonderful cell
A model describes it quite well
Its carbon fixation
Will help out the nation,
The story this paper does tell

The key is the bicarbonate
And making it accumulate.
So once it is home
In the carboxysome,
Fixation occurs at great rate.

Cyanos when out in the wild
Need systems to get carbon piled.
But those parts can pass
From cells grown in flue gas,
So we'll get the genotype dialed.

This photosynthetic machine
Can be trimmed down to make it more lean.
With what we now know
We can make more cells grow,
And will help make the planet more green.

Notation

Variables

C_i^j = variable concentration of species i in phase j, $\frac{\text{mol}}{L}$
D_i^j = diffusivity of species i in phase j, $\frac{m^2}{s}$
Da = Damköhler number
J^* = HCO_3^- flux at carboxysome surface, $\frac{mol}{m^2 \cdot s}$
k_{cat} = carbon fixation rate constant for RuBisCO, s^{-1}
k_f = Rate constant for $CO_2 + OH^- \rightarrow HCO_3^-$, $\frac{L}{\text{mol} \cdot s}$
k_r = Rate constant for $HCO_3^- \rightarrow CO_2 + OH^-$, s^{-1}
$K_{m,i}$ = RuBisCO Michaelis-Menten constant for species i, $\frac{\text{mol}}{L}$
N_{sites} = Total number of RuBisCO sites per cell, sites, sites
r = variable radius, m
R_{Cell} = cell radius, m
R_{Carb} = carboxysome radius, m
$[Ru]_j$ = RuBisCO concentration in phase j, $\frac{\text{sites}}{m^3}$
V_j = volume of phase j, m^3
$v_{\max}$ = maximum active HCO_3^- uptake rate, $\frac{\text{mol}}{L \cdot s}$

Literature Cited

1. Whitton BA, Potts M. *The Ecology of Cyanobacteria: Their Diversity in Time and Space*. Springer; 2000.
2. Tcherkez GGB, Farquhar GD, Andrews TJ. Despite slow catalysis and confused substrate specificity, all ribulose bisphosphate carboxylases may be nearly perfectly optimized. *Proc Nat Acad Sci USA*. 2006;103(19):7246–51.
3. Badger MR, Price GD. CO_2 concentrating mechanisms in cyanobacteria: molecular components, their diversity and evolution. *J Exp Bot*. 2003;54(383):609–622.
4. Price GD, Badger MR, Woodger FJ, Long BM. Advances in understanding the cyanobacterial CO_2-concentrating-mechanism (CCM): functional components, C_i transporters, diversity, genetic regulation and prospects for engineering into plants. *J Exp Bot*. 2008;59(7):1441–61.
5. Butler JN. *Carbon Dioxide Equilibria and their Applications*. 1st ed. Reading, MS: Addison-Wesley Publishing Company Inc.; 1982.
6. Omata T, Takahashi Y, Yamaguchi O, Nishimura T. Structure, function and regulation of the cyanobacterial high-affinity bicarbonate transporter, BCT1. *Funct Plant Biol*. 2002;29(3):151–159.
7. Shibata M, Katoh H, Sonoda M, et al. Genes essential to sodium-dependent bicarbonate transport in cyanobacteria: function and phylogenetic analysis. *J Biol Chem*. 2002;277(21):18658–64.
8. Price GD, Woodger FJ, Badger MR, Howitt SM, Tucker L. Identification of a SulP-type bicarbonate transporter in marine cyanobacteria. *Proc Nat Acad Sci USA*. 2004;101(52):18228–33.
9. Wang H-L, Postier BL, Burnap RL. Alterations in global patterns of gene expression in *Synechocystis* sp. PCC 6803 in response to inorganic carbon limitation and the inactivation of ndhR, a LysR family regulator. *J Biol Chem*. 2004;279(7):5739–51.
10. Ohkawa H, Price GD, Badger MR, Ogawa T. Mutation of ndh genes leads to Inhibition of CO_2 uptake rather than HCO_3^- uptake in *Synechocystis* sp. strain PCC 6803. *J Bacteriol*. 2000;182(9):2591–2596.
11. Shibata M, Ohkawa H, Kaneko T, et al. Distinct constitutive and low-CO_2-induced CO_2 uptake systems in cyanobacteria: genes involved and their phylogenetic relationship with homologous genes in other organisms. *Proc Nat Acad Sci USA*. 2001;98(20):11789–94.
12. Maeda S, Badger MR, Price GD. Novel gene products associated with $NdhD_3/D_4$-containing NDH-1 complexes are involved in photosynthetic CO_2 hydration in the cyanobacterium, *Synechococcus* sp. PCC 7942. *Mol Microbiol*. 2002;43(2):425–35.
13. Klughammer B, Sultemeyer D, Badger MR, Price GD. The involvement of NAD(P)H dehydrogenase subunits, $NdhD_3$ and $NdhF_3$, in high-affinity CO_2 uptake in *Synechococcus* sp. PCC7002 gives evidence for multiple NDH-1 complexes with specific roles in cyanobacteria. *Mol Microbiol*. 1999;32(6):1305–1315.
14. Tanaka S, Kerfeld CA, Sawaya MR, et al. Atomic-level models of the bacterial carboxysome shell. *Science*. 2008;319(5866):1083–6.
15. Yeates TO, Kerfeld CA, Heinhorst S, Cannon GC, Shively JM. Protein-based organelles in bacteria: carboxysomes and related microcompartments. *Nature Rev. Microbiol*. 2008;6(9):681–91.
16. Kinney JN, Axen SD, Kerfeld CA. Comparative analysis of carboxysome shell proteins. *Photosy Res*. 2011;109(1-3):21–32.
17. Shingles R, Moroney JV. Measurement of carbonic anhydrase activity using a sensitive fluorometric assay. *Anal Biochem*. 1997;252(1):190–7.
18. Price GD, Badger MR. Isolation and Characterization of high CO_2-requiring- mutants of the cyanobacterium *Synechococcus* PCC 7942. *Plant Physiol*. 1989:(91)514–525.
19. Price GD, Badger MR. Expression of human carbonic anhydrase in the cyanobacterium *Synechococcus* PCC 7942 Creates a High CO_2-requiring phenotype: evidence for a central role for carboxysomes in the CO_2 concentrating mechanism. *Plant Physiol*. 1989;91(2):505–13.
20. Peña KL, Castel SE, de Araujo C, Espie GS, Kimber MS. Structural basis of the oxidative activation of the carboxysomal γ-carbonic anhydrase, CcmM. *Proc Nat Acad Sci USA*. 2010;107(6):2455–60.
21. Rae BD, Long BM, Badger MR, Price GD. Structural determinants of the outer shell of β-carboxysomes in *Synechococcus elongatus* PCC 7942: roles for CcmK2, K3-K4, CcmO, and CcmL. *PloS One*. 2012;7(8):e43871.
22. Bird RB, Stewart WE, Lightfoot EN. *Transport Phenomena*. 2nd ed. New York, NY: John Wiley and Sons, Inc.; 2007:563–567.
23. Gutknecht J, Bisson M, Tosteson FC. Diffusion of carbon dioxide through lipid bilayer membranes: effects of carbonic anhydrase, bicarbonate, and unstirred layers. *The J Gen Physiol*. 1977;69(6):779–94.
24. Ku S, Edwards G. Oxygen inhibition of photosynthesis. *Planta*. 1978:991–999.
25. Badger MR, Andrews TJ, Whitney SM, et al. The diversity and coevolution of Rubisco, plastids, pyrenoids, and chloroplast-based CO_2-concentrating mechanisms in algae 1. *Can J Bot*. 1998;1071:1052–1071.
26. Bailey J, Ollis DF. Biochemical Engineering Fundamentals. McGraw-Hill Science/Engineering/Math; 1986:928.
27. Kao HP, Abney JR, Verkman a S. Determinants of the translational mobility of a small solute in cell cytoplasm. *J Cell Biol*. 1993;120(1):175–84.
28. Mastro AM, Babich MA, Taylor WD, Keith a D. Diffusion of a small molecule in the cytoplasm of mammalian cells. *Proc Nat Acad Sci USA*. 1984;81(11):3414–8.
29. Wang X, Conway W, Burns R, McCann N, Maeder M. Comprehensive study of the hydration and dehydration reactions of carbon dioxide in aqueous solution. *J Phys Chem A*. 2010;114(4):1734–40.
30. Moronta-Barrios F, Espinosa J, Contreras A. Negative control of cell size in the cyanobacterium *Synechococcus elongatus* PCC 7942 by the essential response regulator RpaB. *FEBS Lett*. 2013;587(5):504–9.
31. Stöckel J, Elvitigala TR, Liberton M, Pakrasi HB. Carbon availability affects diurnally controlled processes and cell morphology of *Cyanothece* 51142. *PloS One*. 2013;8(2):e56887.
32. Liu C, Young AL, Starling-Windhof A, et al. Coupled chaperone action in folding and assembly of hexadecameric RuBisCO. *Nature*. 2010;463(7278):197–202.
33. Xu Y, Tiago Guerra L, Li Z, Ludwig M, Charles Dismukes G, Bryant DA. Altered carbohydrate metabolism in glycogen synthase mutants of *Synechococcus* sp. strain PCC 7002: Cell factories for soluble sugars. *Metabol Eng*. 2012:1–12.
34. Price GD, Sültemeyer D, Klughammer B, Ludwig M, Badger MR. The functioning of the CO_2 concentrating mechanism in several cyanobacterial strains: a review of general physiological characteristics, genes, proteins, and recent advances. *Can J Bot*. 1998;76(6):973–1002.
35. Long BM, Badger MR, Whitney SM, Price GD. Analysis of carboxysomes from *Synechococcus* PCC7942 reveals multiple RuBisCO complexes with carboxysomal proteins CcmM and CcaA. *J Biol Chem*. 2007;282(40):29323–35.
36. Savage DF, Afonso B, Chen AH, Silver P. Spatially ordered dynamics of the bacterial carbon fixation machinery. *Science*. 2010;327(5970):1258–61.
37. Lichtenthaler H. Chlorophylls and carotenoids: Pigments of photosynthetic biomembranes. *Methods Enzymol*. 1987;148:350–382.

Manuscript received Oct. 11, 2013, and final revision received Dec. 3, 2013.